




Salt tolerance in relation to elemental concentrations in leaf cell vacuoles and chloroplasts of a C₄ monocotyledonous halophyte

Takao Oi¹  | Peta L Clode^{2,3}  | Mitsutaka Taniguchi¹  | Timothy D Colmer^{4,5}  | Lukasz Kotula^{4,5} 

¹Graduate School of Bioagricultural Sciences, Nagoya University, Nagoya, Japan

²Centre for Microscopy, Characterisation and Analysis, The University of Western Australia, Perth, Western Australia, Australia

³School of Biological Sciences, The University of Western Australia, Perth, Western Australia, Australia

⁴The UWA School of Agriculture and Environment, The University of Western Australia, Perth, Western Australia, Australia

⁵The UWA Institute of Agriculture, The University of Western Australia, Perth, Western Australia, Australia

Correspondence

Lukasz Kotula, The UWA School of Agriculture and Environment & Institute of Agriculture, The University of Western Australia, 35 Stirling Hwy, Crawley, WA 6009, Australia. Email: lukasz.kotula@uwa.edu.au

Funding information

Japan Society for the Promotion of Science, Grant/Award Number: JP19K15823; Australia Awards Endeavour Fellowship

Abstract

Halophytes accumulate and sequester high concentrations of salt in vacuoles while maintaining lower levels of salt in the cytoplasm. The current data on cellular and subcellular partitioning of salt in halophytes are, however, limited to only a few dicotyledonous C₃ species. Using cryo-scanning electron microscopy X-ray microanalysis, we assessed the concentrations of Na, Cl, K, Ca, Mg, P and S in various cell types within the leaf-blades of a monocotyledonous C₄ halophyte, Rhodes grass (*Chloris gayana*). We also linked, for the first time, elemental concentrations in chloroplasts of mesophyll and bundle sheath cells to their ultrastructure and photosynthetic performance of plants grown in nonsaline and saline (200 mM NaCl) conditions. Na and Cl accumulated to the highest levels in xylem parenchyma and epidermal cells, but were maintained at lower concentrations in photosynthetically active mesophyll and bundle sheath cells. Concentrations of Na and Cl in chloroplasts of mesophyll and bundle sheath cells were lower than in their respective vacuoles. No ultrastructural changes were observed in either mesophyll or bundle sheath chloroplasts, and photosynthetic activity was maintained in saline conditions. Salinity tolerance in Rhodes grass is related to specific cellular Na and Cl distributions in leaf tissues, and the ability to regulate Na and Cl concentrations in chloroplasts.

KEYWORDS

bundle sheath cells, C₄ plant, cellular distribution, cryo-SEM X-ray microanalysis, mesophyll cells, Rhodes grass (*Chloris gayana*), salinity tolerance, transmission electron microscopy, xylem parenchyma

1 | INTRODUCTION

Soil salinity is one of the most significant environmental factors limiting yields of crops and forages (Hillel, 2000). High salt concentration decreases the osmotic potential in the rhizosphere

reducing the capacity of roots to take up water. To cope with low soil water potential induced by salt, plant tissues need to adjust osmotically for maintaining a total solute concentration greater than that in the external solution (Flowers et al., 2015). In halophytes (salt-tolerant plants) and in salt-tolerant nonhalophyte crops (e.g., barley),

This is an open access article under the terms of the Creative Commons Attribution-NonCommercial-NoDerivs License, which permits use and distribution in any medium, provided the original work is properly cited, the use is non-commercial and no modifications or adaptations are made.

© 2022 The Authors. *Plant, Cell & Environment* published by John Wiley & Sons Ltd.

the osmotic adjustment occurs primarily by the accumulation of sodium (Na^+) and chloride (Cl^-) in the tissues (Flowers et al., 2015; Munns et al., 2016). This energy-efficient osmotic adjustment is based on the ability of plants to compartmentalize Na^+ and Cl^- in the vacuoles, which avoids the potential adverse effects on metabolic processes in the cytoplasm (Flowers & Colmer, 2008; Munns et al., 2016). The capacity of vacuolar compartmentation is regarded as the main component of tissue tolerance (Munns et al., 2016). Additionally, Na^+ and Cl^- can be partitioned between different cell types within leaves so that high concentrations of Na^+ and Cl^- are stored in metabolically low-active epidermal cells, but remain relatively low in concentration in photosynthetically active mesophyll cells (James et al., 2006b; Kotula et al., 2019). Once the capacity for storage in vacuoles of epidermal or mesophyll cells is reached, salt entering the cells will begin to accumulate in the cytoplasm and organelles, such as chloroplasts, inducing damage (James et al., 2006b; Kotula et al., 2019; Munns et al., 2016).

Technical limitations have precluded precise definition of threshold levels of Na^+ and/or Cl^- toxicity in various cellular compartments (Cheeseman, 2013). Several reviews have concluded that maximum cytosolic Na^+ concentrations do not exceed 30 mM (Kronzucker & Britto, 2011; Munns & Tester, 2008; Tester & Davenport, 2003). In contrast, the few estimates of the cytosolic concentration of Na^+ in halophytes indicate that nontoxic concentrations could be as high as 150–200 mM (Flowers & Colmer, 2008; Flowers et al., 2015). Similar to the cytosol, chloroplastic Na^+ and Cl^- concentrations have been estimated to be 100–200 mM, even in the presence of >500 mM in the leaf sap (Flowers et al., 2015), suggesting that Na^+ and Cl^- levels in chloroplasts are regulated, which is essential for maintaining high photosynthetic performance in halophytes (Bose et al., 2017). In addition to regulation of Na^+ and Cl^- in various cellular compartments, optimal K^+/Na^+ ratio and maintaining of the cytoplasmic K^+ , Ca^{2+} or Mg^{2+} concentrations are of importance for tissue tolerance (Flowers et al., 2015; Maathuis & Amtmann, 1999; Shabala & Pottosin, 2014). The current data on cellular/subcellular elemental concentrations in halophytes are, however, limited to only a few dicotyledonous species and are based on the analysis of isolated organelles or X-ray microanalysis of leaf mesophyll cells (Flowers et al., 2015). There are no data on cellular/subcellular distributions of Na^+ , Cl^- , K^+ , Ca^{2+} , Mg^{2+} , P or S in halophytes, as far as we are aware.

Rhodes grass (*Chloris gayana* Kunth) belongs to the subfamily Chloridoideae in the Poaceae, is classified as PEP-CK-type C_4 plant and is a halophytic grass (Loch et al., 2004; Santos et al., 2015). It is native to subtropical/tropical Africa, but has been extensively introduced to other subtropical/tropical regions as a pasture/forage because of its high productivity and wide environmental adaptation (Loch et al., 2004; Suttie, 2000). Due to rapid growth, adaptation to a wide range of environmental conditions and substantial genetic diversity both within and between Rhodes grass cultivars (Loch et al., 2004; Negawo et al., 2021), Rhodes grass can be a model C_4 halophytic grass for basic research on salt tolerance mechanism and also used for forage production in some saline areas. The use of

halophytes as models for developing strategies to improve salt tolerance in crops has been suggested by Flowers and Colmer (2008) and Shabala (2013). Salinity tolerance in Rhodes grass has been associated with the ability to excrete excess salt ions on the leaf surfaces via bicellular microhairs (salt glands) on the epidermis of both leaf sides (Lipshitz et al., 1974; Oi et al., 2012, 2013). Rhodes grass also accumulates up to $1500 \mu\text{mol g}^{-1}$ dry weight of Na^+ in leaf tissues (Kobayashi et al., 2007; Oi et al., 2012); however, the physiological mechanisms to cope with high Na^+ and Cl^- concentration within the leaf tissues have not yet been studied in detail.

From the viewpoint of tissue tolerance, we hypothesize that Rhodes grass leaves under high salinity would compartmentalize ions among the cells composing the leaf tissues. Previous studies, using X-ray microanalysis, showed that a relatively salt-tolerant chickpea (salt-sensitive dicot) genotype preferentially accumulated Na in epidermal cells while maintaining low Na in the photosynthetically active mesophyll cells when grown in nutrient solution with 60 mM NaCl (Kotula et al., 2019). In barley (nonhalophyte but salt-tolerant monocot), Na was equally distributed in epidermal and mesophyll cells, but the accumulation of K in mesophyll cells contributed to the maintenance of photosynthetic performance (James et al., 2006b). As far as we are aware, there is no study indicating Na distribution among different cell types in C_4 grasses, which generally possess higher salt tolerance than C_3 grasses. Leaves of C_4 grasses consist of Kranz anatomy, wherein CO_2 is first assimilated by PEPcase in a layer of mesophyll cells that surround an inner layer of bundle sheath cells, where CO_2 is concentrated and refixed by Rubisco (ribulose 1,5-bisphosphate carboxylase/oxygenase) (Sage et al., 2014). Although both mesophyll and bundle sheath cells are photosynthetically active, previous studies of the ultrastructure of chloroplasts indicated that bundle sheath cells are more tolerant to salinity than mesophyll cells; swelling of thylakoids and disruption of envelopes were observed in mesophyll chloroplasts, whereas bundle sheath chloroplasts were hardly damaged in C_4 grasses when grown in soil with 3% NaCl (approx. 520 mM) for 5 days (Omoto et al., 2009, 2010). However, it is unknown whether less damage to bundle sheath than mesophyll chloroplasts was due to lower accumulation of salt in the bundle sheath than mesophyll cells or due to greater tolerance of bundle sheath chloroplasts to Na^+ . It is thus important to clarify the cellular and subcellular concentration of key elements among various cell types of leaf tissues.

The objectives of this study were: (1) to investigate distribution and concentrations of Na, Cl, K, Ca, Mg, P and S in various cell types in Rhodes grass leaves, using cryo-scanning electron microscopy (cryo-SEM) X-ray microanalysis, and link these data to photosynthetic performance; and (2) to investigate elemental concentrations in chloroplasts of mesophyll and bundle sheath cells and report on the effects of salinity on the ultrastructure of chloroplasts. This is the first investigation of cellular and subcellular elemental concentrations in a C_4 halophytic monocot and the first direct comparison of elemental concentrations in chloroplasts of mesophyll and bundle sheath cells and their ultrastructure. So far, cellular/subcellular elemental concentrations have been limited to a few

dicotyledonous species or speculated upon in reviews (e.g., Flowers et al., 2015). Rhodes grass was chosen as it is a widely grown halophytic C_4 forage grass and may be suitable as a C_4 monocot model species for improving knowledge on salinity tolerance, with a potential application in developing future crops. We tested the following hypotheses: (1) for plants grown in saline media, Na is preferentially accumulated in epidermal cells of leaves, but is maintained at low levels in photosynthetically active mesophyll and/or bundle sheath cells, while the opposite is found for K; (2) concentration of Na in chloroplasts is regulated, that is, Na is maintained at lower levels than in respective vacuole; and (3) allocation of other elements (Ca or P) in various cells of the leaf is linked to osmotic/charge balance.

2 | MATERIALS AND METHODS

2.1 | Plant material and growth conditions

Caryopses of Rhodes grass (*Chloris gayana* Kunth, cv. Katambora) were washed in aerated 0.5 mM $CaSO_4$ for 3 h and then placed on plastic mesh floating on aerated 25% strength nutrient solution (see below for composition) in the dark at 30°C for germination. On Day 4, seedlings were exposed to sunlight in a glasshouse with temperatures of 30°C/25°C day/night (July–August in Perth, Australia) and the nutrient solution was changed to 50% strength. On Day 12, six plants were transferred to each 4.5 L pot containing 100% strength nutrient solution. On Day 18, the NaCl treatments were imposed in steps of 50 mM (see below). The composition of the nutrient solution was (mM): K^+ , 5.95; Ca^{2+} , 1.5; Mg^{2+} , 0.4; NH_4^+ , 0.625; NO_3^- , 4.375; SO_4^{2-} , 1.9; $H_2PO_4^-$, 0.2, and also Na^+ , 0.2; SiO_3^{2-} , 0.1; and the micronutrients (μM): Cl^- , 50; B, 25; Mn^{2+} , 2; Zn^{2+} , 2; Ni^{2+} , 1; Cu^{2+} , 0.5; Mo 0.5; Fe-EDTA, 50. The solution was buffered with 1 mM MES (2-[N-morpholino] ethanesulfonic acid) and pH was adjusted to 6.5 using KOH (to give the final K^+ concentration as above). A small dose of $FeSO_4$ (5 μM) was given at the seedling stage, to prevent any possible Fe deficiency that can otherwise occur. The solution in all pots was renewed weekly.

2.2 | Treatments and sampling procedure

Three treatments were applied (18 days after seeds were imbibed): nonsaline control (containing 0.2 mM Na^+ and 0.05 mM Cl^- ; see above), and either 100 or 200 mM NaCl. The saline treatments were imposed by the addition of 50 ml of 4.3 M NaCl stock solution to each 4.5 L pots (volume of solution was 4.3 L) to gradually raise the NaCl concentration by 50 mM NaCl steps at 12 h intervals to the final concentrations of 100 or 200 mM (NaCl was imposed in steps at the first treatment imposition, but was added to the nutrient solution at a final concentration of either 0, 100 or 200 mM at the time of each subsequent weekly nutrient solution renewal). There were four replicate pots for each treatment. Pots were in randomized design and were re-randomized at

the time of each nutrient solution renewal to minimize the effects of any possible environmental gradients within the glasshouse. Immediately before treatments were imposed, the initial samples of two plants were taken from each pot, so that four plants remained in each pot. The subsequent samples of two plants per pot were taken at 15–17 and 24 days after the first addition of 50 mM NaCl (33–35 and 42 days after imbibition of seeds). All measurements or samplings for leaves were conducted on leaf-blades and not on leaf sheaths; blades (i.e., lamina) and sheath were clearly distinguishable with the line called lamina joints. Roots and shoot bases of plants from the 100 and 200 mM NaCl treatments were rinsed three times, for 30 s each time, respectively, with 200 and 400 mM mannitol + 4 mM $CaSO_4$, and plants from the nonsaline controls were rinsed in 4 mM $CaSO_4$. The fresh weights of various plant parts (roots, green shoots and dead leaves) were recorded, dried at 70°C for 72 h and then the dry weights were recorded (Figures S1 and S2).

2.3 | Leaf gas exchange and chlorophyll fluorescence measurements

All measurements were conducted on the second youngest fully expanded leaf-blades of one of the two plants just before sampling at 16 and 17 days of treatments (see above), using an open gas exchange system coupled with a 20 mm² chamber head fluorometer (LI-6400XT; LI-COR Biosciences). Net photosynthetic rate (A), intercellular CO_2 concentration (C_i), stomatal conductance to water vapour (g_s) and transpiration rate (T) were determined at a photosynthetically active radiation of 1500 μmol photons $m^{-2} s^{-1}$ (light saturated; Basu et al., 2007), leaf chamber temperature of $30 \pm 1^\circ C$, relative humidity of 55%–65% and CO_2 concentrations of 400 $\mu mol mol^{-1}$ (ambient). The measurements were taken between 11.00 and 16.00 h.

For determination of the maximum quantum efficiency of photosystem II reaction centres (F_v/F_m), minimal fluorescence level (F_o) was measured using a modulated pulse (<0.05 μmol photons $m^{-2} s^{-1}$ for 1.8 μs), which was sufficiently low not to induce any significant variable fluorescence, while maximal fluorescence level (F_m) was determined by a saturating flash of light (7000 μmol photons $m^{-2} s^{-1}$ for 0.8 s) in the dark-adapted leaves (30 min). Variable fluorescence, F_v , is the difference between F_o and F_m .

2.4 | Leaf osmotic potential measurements

Osmotic potential measurements were conducted on the second youngest fully expanded leaves of one of the two plants sampled at 16 days of treatments. Fifty millimetres of the middle part of the leaf-blade was collected into an air-tight cryo-vial, frozen in liquid nitrogen and kept at $-20^\circ C$. Leaf samples were thawed in the vials and then crushed to obtain a sample of tissue sap. The osmotic potential (or 'solute potential', Ψ_s) was measured using 20 μl of sap in a calibrated freezing-point depression osmometer (Model 210; Fiske Associates).

2.5 | Excreted and tissue ion analyses

The blades of the sixth leaf were used for ion analyses. At 11 days after treatment imposition, the blades of the sixth leaf were thoroughly washed with deionized water to remove salts and other contaminants from the surfaces. At 15 days after treatment imposition (4 days after washing), the blades from the sixth leaf were excised and inserted into tubes containing 20 ml of distilled water and shaken for 30 s to remove excreted ions from the surface. The leaf-blades were then removed and dried at 70°C for 72 h, and the dry weights were recorded. Oven-dried leaf-blades and tissues (whole shoots, whole roots) were ground to a fine powder in a ball-mill grinder (2010 Geno/Grinder; SPEX SamplePrep) or a blade grinder (CG2B 2010; Breville) and then extracted in 0.5 M HNO₃ (Munns et al., 2010). The rinsing and extracting solutions were analysed for Na⁺ and K⁺ using a flame photometer (Model 410; Sherwood Scientific) and Cl⁻ using a chloridometer (Model 50CL; SLAMED) (Figures S3 and S4).

2.6 | Light microscopy for leaf anatomy

Segments (~5 × 5 mm) from the sixth fully expanded leaf-blades were collected after 15 days of treatments and fixed with 2.5% glutaraldehyde in 0.1 M phosphate buffer for 24 h before being stored at 4°C. After rinsing in deionized water, fixed leaf segments were dehydrated in graded series of acetone (25, 50, 75 and 95%) and then infiltrated and embedded in glycol methacrylate. Four-μm-thick sections were cut with a Sorvall microtome equipped with a glass knife, stained for 1 min in 0.05% (w/v) toluidine blue O in benzoate buffer at pH 4.4, washed and air-dried. Sections were viewed under white light and photographed using a microscope (Axioskop2 Plus; Zeiss) equipped with a digital camera (Axiocam; Zeiss).

2.7 | Transmission electron microscopy (TEM) for leaf anatomy

Segments (~2 × 2 mm) from the middle part of the sixth fully expanded leaf-blades were collected after 15 days of treatments and fixed as described above. Samples were then prepared as described in detail in Kotula et al. (2019). Briefly, after washing in phosphate buffer, leaf segments were postfixed in 1% OsO₄ in 0.1 M phosphate buffer, rinsed in deionized water and dehydrated in graded series of ethanol, followed by anhydrous acetone. Leaf segments were then infiltrated and embedded in a Procure-Araldite epoxy resin mixture. Ultrathin sections (100 nm thick) were cut with a diamond knife, placed on copper grids and double-stained with 2% uranyl acetate for 20 min, followed by lead citrate for 4 min. The specimens were then observed with a TEM (H-7500; Hitachi) at an accelerating voltage of 100 kV, and photographed with a CCD camera (Advanced Microscopy Technique) connected to the microscope.

2.8 | Scanning electron microscopy (SEM) for leaf anatomy

Segments (~2 × 2 mm) from the middle part of the sixth fully expanded leaf-blades were prepared and embedded in resin as described above for TEM. Semi-thin sections (500 nm thick) were cut using a diamond knife with a large water trough, placed on a glass slide, double-stained with uranyl acetate and lead citrate and dried. The uncoated specimens were observed and imaged with a low vacuum SEM (TM3000; Hitachi) using backscattered electrons and an accelerating voltage of 15 kV.

2.9 | Cell-specific element analysis by cryo-SEM X-ray microanalysis

Small segments (~3 × 2 mm) of leaf-blades were excised from the middle part of the sixth fully expanded leaves at 15 days of treatments, placed on an aluminium grooved pin with optimal cutting temperature compound and plunge frozen into liquid nitrogen, thereby immediately immobilizing and preserving cellular ions (Hayes et al., 2018; Kotula et al., 2019). Samples were prepared and analysed as described in detail in Hayes et al. (2018).

Briefly, frozen-hydrated, cryo-planed samples were coated with 20 nm chromium and transferred under vacuum to a field emission SEM (Supra 55VP; Zeiss). Samples were analysed at -150°C at an accelerating voltage of 15 kV and a 2 nA beam current in high-current mode, with a beam calibration conducted before each analysis using a pure Cu standard. All analysis and quantification were performed using an X-Max80 SDD X-ray detector interfaced to an AZtecEnergy software (Oxford Instruments), with all elements analysed, except for H (set to 11.11%), N (set to 3.3%) and O (analysed by difference). For Na quantitation, pulse pile-up correction is required due to the high number of O X-rays generated in frozen-hydrated biosamples. This correction factor was determined empirically by analysing Na standards of known concentration and is automatically applied to the quantitation calculations by the software. This AZtec system has been shown to be highly suited to the analysis of frozen-hydrated biomaterials with accurate quantitation obtained using in-built standards, superior correction factors and commercial algorithms (Marshall, 2017). Cryo-SEM-energy-dispersive X-ray microanalysis (cryo-SEM-EDS) typically allows accurate, fully quantitative analyses to be performed at the micron-scale for most biologically relevant elements. As the sample is simply rapidly frozen and then cryo-planed, loss or redistribution of mobile ions is effectively eliminated, and modern cryo-systems allow both rapid preparation and mapping (=data in a few hours). Important considerations for analysis include freezing quality/ice crystal damage, sample flatness/topography effects on X-ray signals, peak overlaps/pile up and element detection limits (~few mmol kg⁻¹). Measurements of individual cells were conducted in the area occupied by vacuole for the upper epidermal (UE) cells,

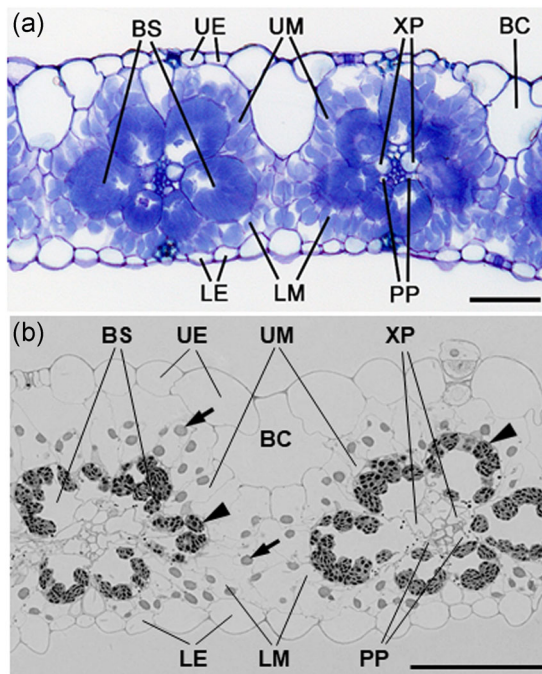


FIGURE 1 Optical image (a) and scanning electron micrograph (b) of cross-sections of leaf-blade of the sixth fully expanded leaves of Rhodes grass indicating typical cell types and chloroplasts that were analysed to give cellular concentration profiles. (a) Sections were stained with toluidine blue O and viewed with a bright field. (b) Arrowheads indicate chloroplasts in bundle sheath cells that are in a centrifugal position to the vascular tissue; arrows indicate chloroplasts in mesophyll cells that are distributed in the cell periphery. Plants were grown in aerated nonsaline nutrient solution for 16 days after the treatments had been imposed. BC, bulliform cell; BS, bundle sheath; LE, lower (abaxial) epidermis; LM, lower mesophyll; PP, phloem parenchyma; UE, upper (adaxial) epidermis; UM, upper mesophyll; XP, xylem parenchyma. Scale bars = 50 μm

bulliform cell (BC) in the upper epidermis, upper mesophyll (UM) cells, bundle sheath (BS) cells, xylem parenchyma (XP), phloem parenchyma (PP), lower mesophyll (LM) cells, and lower epidermal (LE) cells (Figure 1). In addition, the analytical resolution of the technique ($\sim 2 \mu\text{m}$ under conditions used) was sufficient for elemental analyses of large chloroplasts in mesophyll cells and in bundle sheath cells. Spectra were collected from each cell type from three different leaf-blades from three different replicate plants. Concentration data are generated as weight % and converted to mmol kg^{-1} wet weight.

2.10 | Statistical analyses

Data are presented as means \pm SE. One- or two-way analysis of variance (with Tukey's multiple comparison test) was used to compare means or to assess the effects of treatment, cell type or treatment \times organelle type interactions. GraphPad Prism (version 9.02; Graph-Pad Software) was used to prepare graphs and for statistical analysis.

3 | RESULTS

3.1 | Elemental concentration in various cell types of leaf-blades

The transversal leaf-blade sections of Rhodes grass (Figure 1) show a typical Kranz anatomy of the PCK-type C_4 grasses with vascular bundle surrounded by bundle sheath cells, which are further surrounded by radially arranged mesophyll cells in both leaf sides. The bundle sheath cells contained large chloroplasts located on the centrifugal position to the vascular tissue, and the chloroplasts in mesophyll cells were smaller than those in bundle sheath cells and were arranged randomly in the cell periphery. In the vascular bundle, the xylem parenchyma and phloem parenchyma cells were adjacent to bundle sheath cells. In the epidermis, large bulliform cells were located on the adaxial surface between the veins (Figure 1). Measurements of the cellular concentration of Na, Cl, K, Ca, Mg, S and P on the transversal section of leaf-blades of the sixth fully expanded leaves were conducted in the area occupied by vacuole in the upper and lower epidermis, bulliform cells, upper and lower mesophyll cells, bundle sheath cells, and xylem parenchyma and phloem parenchyma cells (Figure 1). The elemental concentrations in chloroplasts were measured for upper mesophyll and lower mesophyll and bundle sheath cells.

3.1.1 | Sodium

In plants from nonsaline control pots, vacuolar Na concentrations [Na] did not exceed 21 mM, with the exception of xylem parenchyma (61 mM), in various cells types across the transverse section of leaf-blades (Figures 2 and 3a). The 200 mM NaCl treatment drastically increased vacuolar [Na] in all cells; however, the [Na] considerably differed among the various cell types (Figure 3a). The [Na] was similar in the upper and lower epidermal cells and bulliform cells, with an average of 382 mM; it was ~ 307 mM in upper and lower mesophyll cells, but it dropped to 195 mM in bundle sheath cells being about 51% and 64% as compared to epidermal and mesophyll cells, respectively. [Na] was the highest in xylem parenchyma (529 mM) (visible as two accumulated parts in each vein in Figure 2), and it was 227 mM in phloem parenchyma.

Similar to [Na] in the vacuoles, [Na] in the chloroplasts of mesophyll and bundle sheath cells were low in nonsaline control plants (average of 19 mM) (Figures 4a and S5). The imposition of 200 mM NaCl treatment increased [Na] in the chloroplasts of both mesophyll (3.0-fold of nonsaline control) and bundle sheath cells (4.8-fold of nonsaline control); however, the increases were markedly lower as compared to those in the respective vacuoles (~ 18 -fold of nonsaline controls for both mesophyll and bundle sheath cells). As a result, [Na] in the chloroplasts of plants grown in 200 mM NaCl was 90 mM in mesophyll (compared to 307 mM in vacuoles) and 34 mM in bundle sheath cells (compared to 195 mM in vacuoles) (Figures 4a and S5).

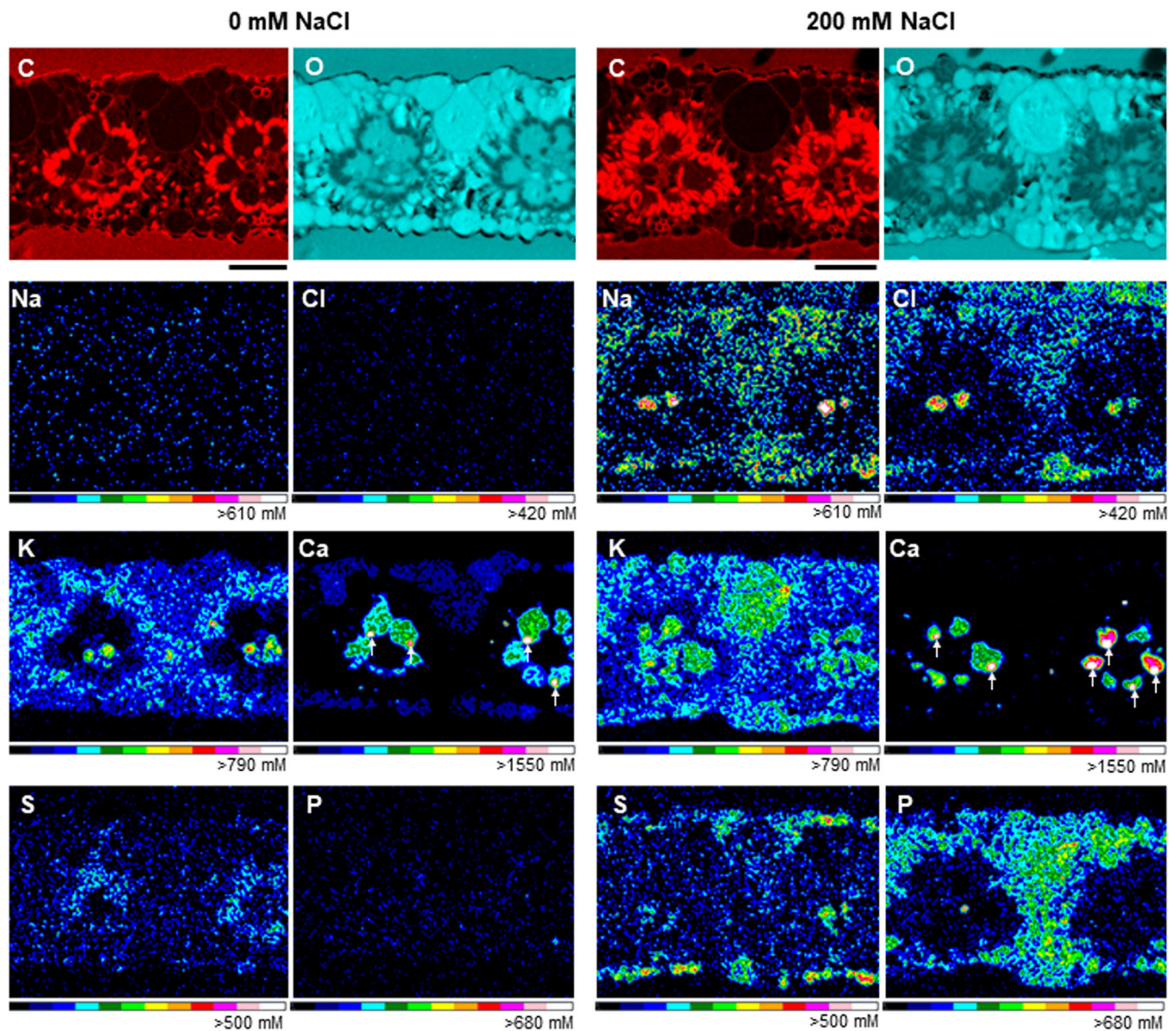


FIGURE 2 Quantitative element maps of Na, Cl, K, Ca, S and P from the cryo-planed, frozen-hydrated leaf-blades of the sixth fully expanded leaves of Rhodes grass. Qualitative maps of C and O are included to show leaf structure. Plants were grown in aerated nutrient solution with 0 (nonsaline control) or 200 mM NaCl for 16 days. Treatments were imposed on 18-day-old plants. Elemental concentrations from different cell types are summarized in Figures 3 and 4. Magnified views of element maps indicating areas occupied by chloroplasts in the upper mesophyll or bundle sheath cells are presented in Figure S5. For these maps, the concentrations (in mM) are scaled to best reveal element variations across cell layers and treatments, with black = 0 (below detection, approximately <3 mM) for all maps, and white >610 mM for Na, >420 mM for Cl, >790 mM for K, >1550 mM for Ca, >500 mM for S, and >680 mM for P. The changes in concentration along the colour scale are linear. Arrows in Ca maps indicate regions of high concentrations of Ca, presumably Ca-based crystals. Scale bar for all images = 50 μ m. Quantitative element maps of Mg are presented in Figure S6a, b [Color figure can be viewed at wileyonlinelibrary.com]

3.1.2 | Chloride

The distribution pattern of Cl in the leaf-blades was similar to that of Na (Figures 2 and 3b). In nonsaline control plants, Cl concentrations [Cl] were low in all cells and ranged from 2 mM in bundle sheath cells to 19 mM in phloem parenchyma (Figure 3b). The 200 mM NaCl treatment drastically increased [Cl] in all cells; however, the [Cl] in respective cells were 49%–82% lower than

[Na] (Figure 3a). In plants grown in 200 mM NaCl, the [Cl] was similar in the upper and lower epidermal cells and bulliform cells, with an average of 138 mM; it was ~76 mM in upper and lower mesophyll cells and in phloem parenchyma, whereas the [Cl] was the lowest in the bundle sheath cells with 34 mM (about 25% and 49% as compared to epidermal and mesophyll cells, respectively) and it reached the highest concentrations of 270 mM in xylem parenchyma.

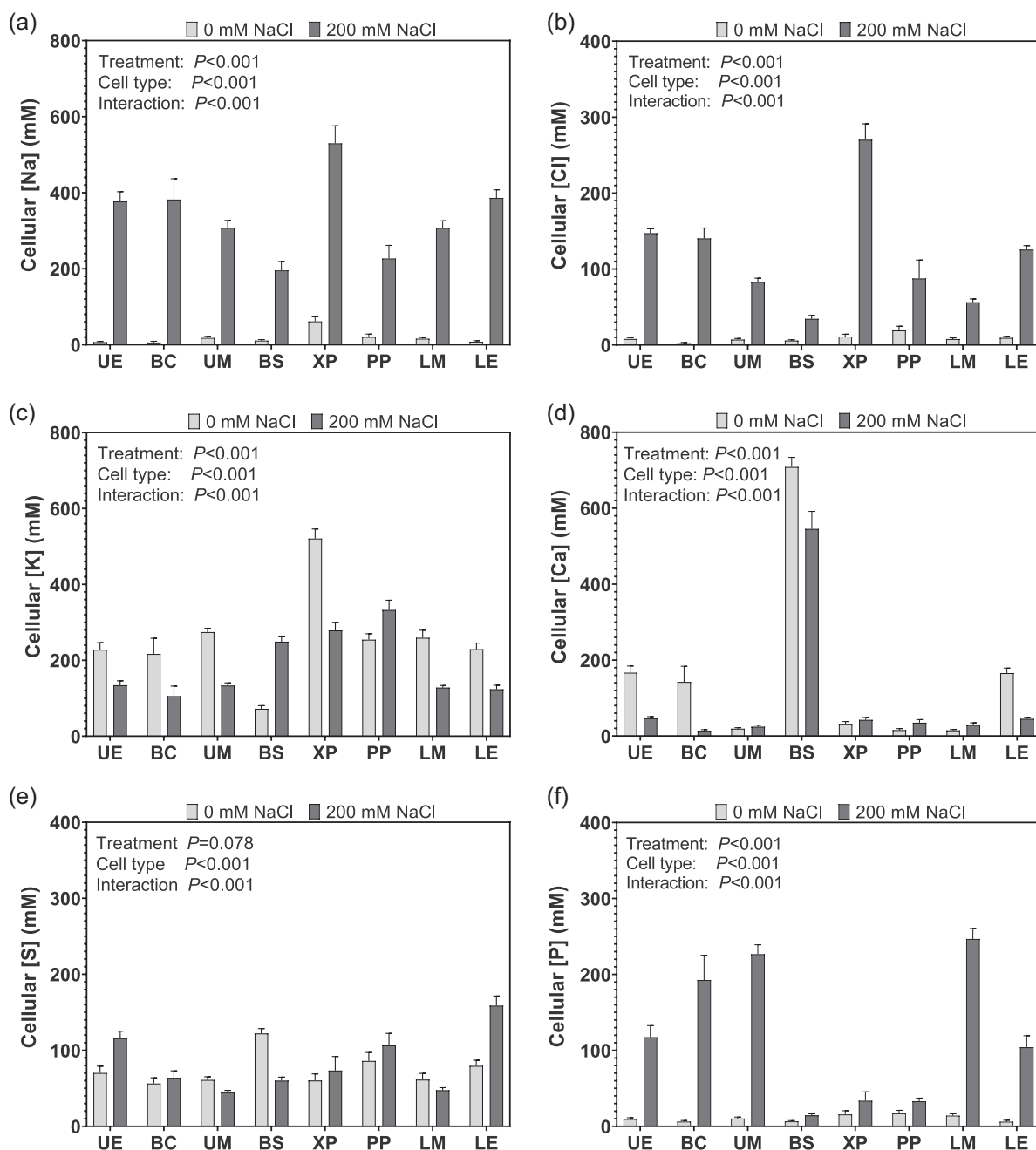
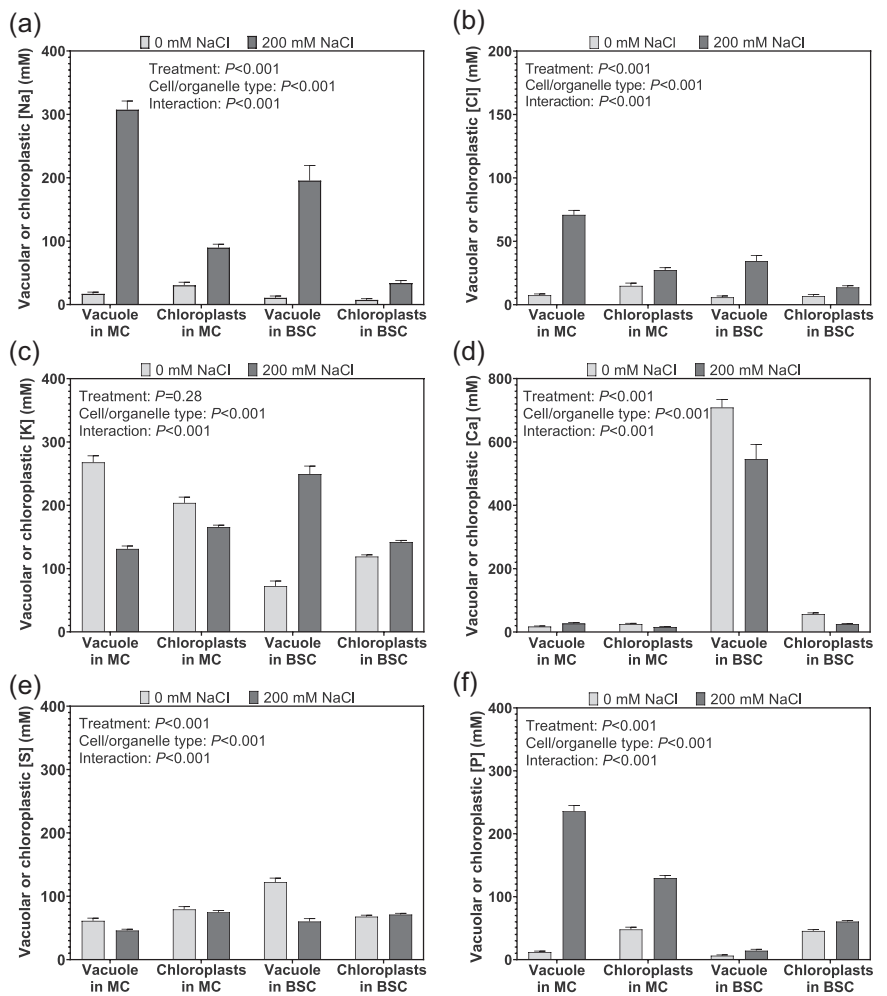


FIGURE 3 Cellular concentrations of Na (a), Cl (b), K (c), Ca (d), S (e) and P (f) in various cell types in the leaf-blades of fully expanded sixth leaves of Rhodes grass grown in aerated nutrient solution with 0 (nonsaline control) or 200 mM NaCl for 16 days. Treatments were imposed on 18-day-old plants. Elemental concentrations were measured by cryo-scanning electron microscopy X-ray microanalysis. The concentrations in mM (mmol kg^{-1} water) are per unit fresh weight from fully hydrated, cryo-fixed cells. Data are means \pm SE ($n = 15\text{--}80$ cells measured for three to four leaf-blades each across a different replicate plant). The results of a two-way analysis of variance are given in each panel. BC, bulliform cell; BS, bundle sheath cells; LE, lower (abaxial) epidermis; LM, lower mesophyll; PP, phloem parenchyma; UE, upper (adaxial) epidermis; UM, upper mesophyll; XP, xylem parenchyma. Cellular concentrations of Mg are presented in Figure S6c

Similar to [Cl] in the vacuoles, [Cl] in the chloroplasts of mesophyll and bundle sheath cells were low in leaf-blade cells of nonsaline control plants (average of 11 mM) (Figures 4b and S5). The imposition of 200 mM NaCl treatment increased the [Cl] in the chloroplasts of both mesophyll cells (1.8-fold of controls) and bundle sheath cells (2.0-fold of controls); however, the increases

were markedly lower as compared to those in their respective vacuoles (9.6-fold and 5.9-fold of controls in mesophyll and bundle sheath cells, respectively). As a result, [Cl] in the chloroplasts of plants grown in 200 mM NaCl was 27 mM in the mesophyll (71 mM in vacuoles) and 13 mM in bundle sheath cells (34 mM in vacuoles) (Figures 4b and S5).

FIGURE 4 Concentrations of Na (a), Cl (b), K (c), Ca (d), S (e) and P (f) in vacuole and chloroplasts of mesophyll and bundle sheath cells in the leaf-blades of the sixth fully expanded leaves of Rhodes grass grown in aerated nutrient solution with 0 (nonsaline control) or 200 mM NaCl for 16 days. Treatments were imposed on 18-day-old plants. Elemental concentrations were measured by cryo-scanning electron cryomicroscopy X-ray microanalysis. The concentrations in mM (mmol kg^{-1} water) are per unit fresh weight from fully hydrated, cryo-fixed cells. Data are means \pm SE ($n = 44\text{--}146$ regions measured for three to four leaf-blades each across a different replicate plant). The results of a two-way analysis of variance are given in each panel.; BSC, bundle sheath cells; MC, mesophyll cells. Concentrations of Mg in vacuole and chloroplasts are presented in Figure S6d



3.1.3 | Potassium

In leaf-blades of nonsaline control plants, K concentrations [K] in vacuoles were similar in the majority of cells, with an average of 244 mM in upper and lower epidermal cells, bulliform cells, upper and lower mesophyll cells, and phloem parenchyma. [K] was the lowest in bundle sheath cells (72 mM) and the highest in xylem parenchyma (521 mM) (Figures 2 and 3c). The 200 mM NaCl treatment decreased [K] to about 50% of controls in epidermal, bulliform cells, mesophyll (average of 125 mM) and xylem parenchyma (279 mM) cells. By contrast, [K] increased 3.4-fold in bundle sheath cells reaching 249 mM and it was 333 mM in phloem parenchyma (Figures 2 and 3c).

In nonsaline control plants, [K] in the chloroplasts of mesophyll cells was 1.7-fold higher as compared to the [K] in the chloroplasts of bundle sheath cells (Figures 4c and S5). When compared to their respective vacuoles, chloroplast [K] was 25% lower (204 mM) than vacuolar [K] (268 mM) in mesophyll cells, but in bundle sheath cells, chloroplast [K] was 1.6-fold higher (119 mM) than [K] in the vacuole (72 mM). The 200 mM NaCl treatment decreased the chloroplast [K] in mesophyll cells to 82% (165 mM) of the nonsaline control, but it increased 1.6-fold the chloroplast [K] in bundle sheath cells (142 mM), as compared to nonsaline controls (albeit the mean was

not statistically different) (Figures 4c and S5). Similarly to chloroplasts, as compared to nonsaline controls, the 200 mM NaCl treatment decreased the vacuolar [K] in mesophyll cells to 49% (131 mM), but it increased 3.4-fold the vacuolar [K] in bundle sheath cells (249 mM) (Figure 4c).

3.1.4 | K:Na ratio

In leaf-blades of nonsaline control plants, the K:Na ratio in vacuoles was similar in the majority of cells ranging from 127:1 to 190:1 in epidermal, bulliform cells, mesophyll and phloem parenchyma cells, but it was on average 41:1 in bundle sheath and xylem parenchyma cells (Table 1). The 200 mM NaCl treatment did not affect the K:Na ratio in bundle sheath cells (32:1), but it reduced the K:Na ratio in other cells to an average of 0.78:1.

In nonsaline control plants, the K:Na ratio in the chloroplasts of mesophyll cells was 1.4-fold higher than that in the chloroplasts of bundle sheath cells, which was 103:1 and 75:1, respectively (Table 2). The 200 mM NaCl treatment decreased the K:Na ratio in chloroplasts of both mesophyll and bundle sheath cells to 14:1 and 22:1, respectively. As a result, the K:Na ratio in chloroplasts was 24-fold

TABLE 1 K:Na ratio in various cell types in the leaf-blades of the sixth fully expanded leaves of Rhodes grass

Cell type	Treatment	
	Control	200 mM NaCl
Upper epidermis	166 ± 21	0.5 ± 0.1
Bulliform cell	190 ± 43	0.4 ± 0.2
Upper mesophyll	173 ± 19	0.6 ± 0.1
Bundle sheath cell	37 ± 7	32.2 ± 13.3
Xylem parenchyma	45 ± 25	0.7 ± 0.1
Phloem parenchyma	129 ± 34	2.2 ± 0.3
Lower mesophyll	127 ± 20	0.5 ± 0.0
Lower epidermis	170 ± 21	0.4 ± 0.0

Note: Plants were grown in aerated nutrient solution with 0 (nonsaline control) or 200 mM NaCl treatment for 16 days. Treatments were imposed on 18-day-old plants. Elemental concentrations were measured by cryo-SEM X-ray microanalysis. Data are means ± SE ($n = 15$ –80 cells measured across three to four different leaf-blades each from a different replicate plant). There were significant effects of treatment, cell type, and treatment × cell type interaction at $p < 0.001$ (two-way ANOVA).

Abbreviations: ANOVA, analysis of variance; cryo-SEM, cryo-scanning electron microscopy; K:Na, potassium:sodium.

TABLE 2 K:Na ratio in vacuole and chloroplasts of mesophyll and bundle sheath cells in the leaf-blades of the sixth fully expanded leaves of Rhodes grass

Cell type	Treatment	
	Control	200 mM NaCl
Vacuole in MC	153 ± 16	0.6 ± 0.1
Chloroplasts in MC	103 ± 11	13.7 ± 1.1
Vacuole in BSC	37 ± 6	32.2 ± 4.4
Chloroplasts in BSC	75 ± 11	21.9 ± 3.0

Note: Plants were grown in aerated nutrient solution with 0 (nonsaline control) or 200 mM NaCl treatment for 16 days. Treatments were imposed on 18-day-old plants. Elemental concentrations were measured by cryo-SEM X-ray microanalysis. Data are means ± SE ($n = 44$ –146 locations measured across three to four different leaf-blades each from a different replicate plant). There were significant effects of treatment, cell/organelle type, and treatment × cell/organelle type interaction at $p < 0.001$ (two-way ANOVA).

Abbreviations: ANOVA, analysis of variance; BSC, bundle sheath cells; cryo-SEM, cryo-scanning electron microscopy; K:Na, potassium:sodium; MC, mesophyll cells.

higher than that in the vacuole of mesophyll cells, but the vacuolar and chloroplast K:Na were similar in bundle sheath cells.

3.1.5 | Calcium

In leaf-blades of nonsaline control plants, Ca accumulated to the highest concentrations in bundle sheath cells (708 mM); it was on average 160 mM in epidermal cells and bulliform cells, and did not exceed

32 mM in other cell types (Figures 2 and 3d). The 200 mM NaCl treatment decreased [Ca] in the vacuoles of bundle sheath cells to 77% of controls and to about 20% of controls in epidermal and bulliform cells, whereas [Ca] in mesophyll cells and xylem parenchyma and phloem parenchyma cells were not affected by the NaCl treatment. As a result, [Ca] remained high in bundle sheath cells (545 mM), but was low, with an average of 34 mM, in other cell types (Figure 3d).

The [Ca] of chloroplasts were similar in both mesophyll and bundle sheath cells, with an average of 30 mM in both nonsaline control and 200 mM NaCl treatments (Figures 4d and 55). It should be noted that regions of high [Ca]—presumably Ca-based crystals (Ca maps in Figures 2 and 55)—were carefully excluded from analyses.

3.1.6 | Sulphur

In leaf-blades of nonsaline control plants, S concentration [S] in the vacuole was the highest in bundle sheath cells with 122 mM, but ranged from 56 to 86 mM in other cell types (Figures 2 and 3e). The 200 mM NaCl treatment increased vacuolar [S] to 115 mM in the upper epidermal cells (1.6-fold increase as compared to nonsaline control) and to 158 mM in the lower epidermal cells (2-fold increase). By contrast, the [S] dropped to 60 mM in bundle sheath cells (49% of controls) and was not affected in other cell types ranging from 44 mM in upper mesophyll cells to 107 mM in phloem parenchyma cells (Figure 3e).

The [S] in the chloroplasts of mesophyll and bundle sheath cells were similar, with an average of 73 mM in both nonsaline control and 200 mM NaCl treatment (Figures 4e and 55).

3.1.7 | Phosphorus

In leaf-blades of nonsaline control plants, P concentrations [P] in the vacuole were low in all cells and did not exceed 17 mM (Figures 2 and 3f). The 200 mM NaCl treatment increased [P] to on average 111 mM in epidermal cells and 222 mM in bulliform cells and mesophyll cells, but [P] remained low, with an average of 27 mM in bundle sheath cells and xylem parenchyma and phloem parenchyma cells.

In leaf-blades of nonsaline controls, the [P] in chloroplasts of mesophyll and bundle sheath cells was on average 47 mM, which was, respectively, 4-fold and 7-fold higher as compared to [P] in their respective vacuoles (Figures 4f and 55). The 200 mM NaCl treatment increased [P] of chloroplasts to 129 mM in mesophyll cells, but in bundle sheath cells, the [P] remained similar to that in nonsaline control (61 mM).

Concentrations of Mg in various cell types are presented in Figure S6.

3.2 | Ion concentrations in leaf-blades

Nonsaline controls had low average leaf-blade [Na^+] (8.5 mM). The imposition of 100 or 200 mM treatments increased the leaf-blade [Na^+] to 178 or 240 mM, respectively (Figure S4a). Similarly

to $[Na^+]$, nonsaline controls had low leaf-blade $[Cl^-]$, with an average of 7 mM, and the imposition of either 100 or 200 mM NaCl increased the leaf-blade $[Cl^-]$ to 135 or 156 mM, respectively (Figure S4a). The $[K^+]$ showed the reverse pattern to that of leaf $[Na^+]$ and $[Cl^-]$, with leaf-blade $[K^+]$ being the highest in nonsaline control plants (191 mM) and decreasing in 100 and 200 mM NaCl-treated plants to 129 or 151 mM, respectively (Figure S4a). The K:Na ratio in the leaf-blades of plants in nonsaline nutrient solution was 23:1, and it decreased to 0.74:1 in 100 mM and to 0.64:1 in 200 mM NaCl treatments (Table S1). The ion concentrations in leaf-blades on a dry weight basis and that in shoots on both tissue water and dry weight basis are shown in Figure S4. Excretion rates of Na^+ , Cl^- and K^+ from the leaf-blade are presented in Figure S3.

3.3 | Effect of NaCl on chloroplast ultrastructure in mesophyll and bundle sheath cells

There was no notable difference in the ultrastructure of chloroplasts in mesophyll cells of the sixth leaves of plants in nonsaline control and 200 mM treatments (Figure 5a–d). In both treatments, mesophyll chloroplasts showed similar ellipse shape (4–6 μm in length and 2–3 μm in width) and possessed fine thylakoid membranes and tall granum stacks, several plastoglobules but without starch granules (Figure 5c,d). The bundle sheath chloroplasts were larger and more numerous than mesophyll chloroplasts in both nonsaline and 200 mM NaCl treatments (Figure 5a–b). The chloroplasts in both cell types possessed well-organized stroma thylakoid membranes and granum stacks, but those in bundle sheath cells were shorter as compared to those in mesophyll cells,

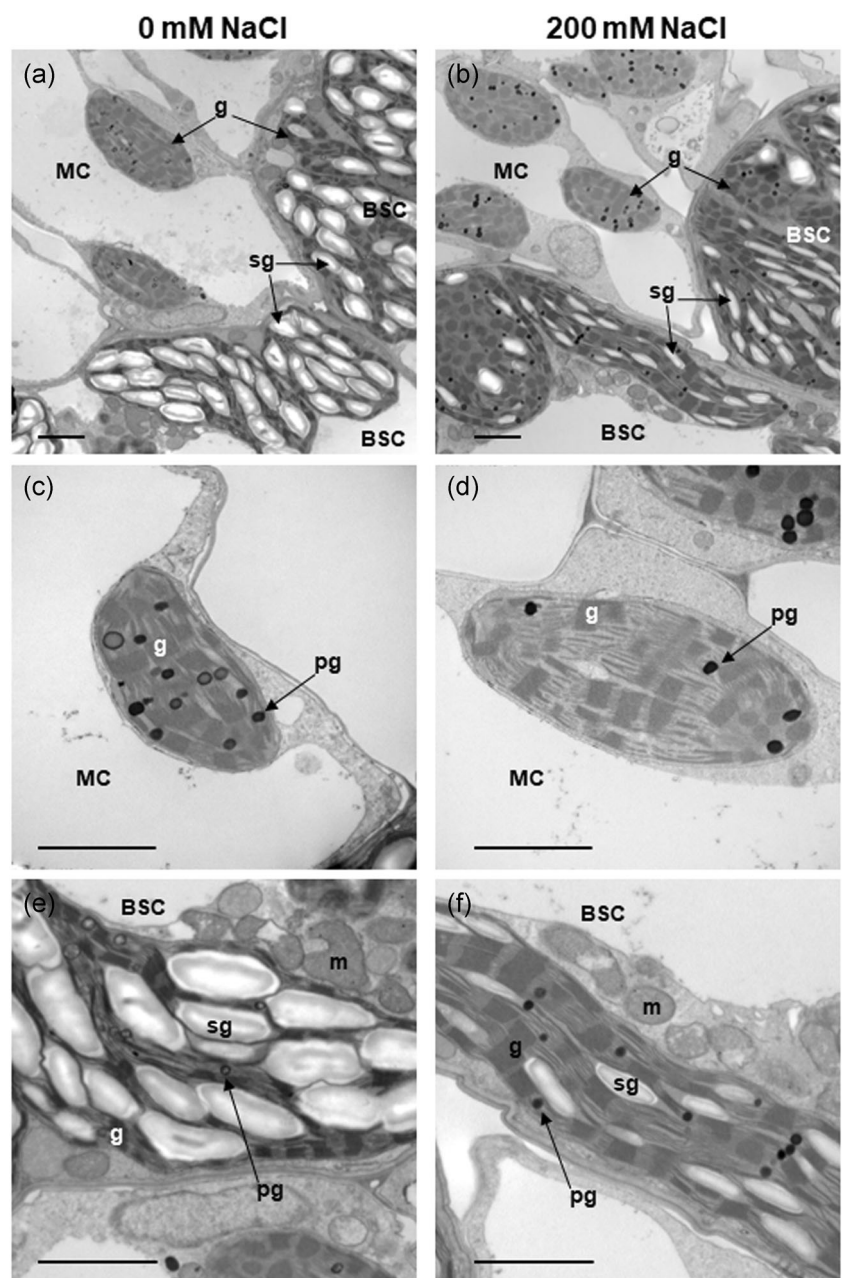


FIGURE 5 Transmission electron micrographs of chloroplasts ultrastructure in mesophyll and bundle sheath cells in the leaf-blade of the sixth leaves of Rhodes grass grown in aerated nutrient solution with 0 mM (nonsaline control) (a,c,e) and 200 mM NaCl (b,d,f) for 16 days. Treatments were imposed on 18-day-old plants. Magnified view of chloroplasts in mesophyll cells (c,d) and bundle sheath cells (e,f). Images are typical of structures seen across three replicate leaf-blades. BSC, bundle sheath cell; g, granum; m, mitochondrion; MC, mesophyll cells; pg, plastoglobule; sg, starch granule. Scale bars = 2 μm

but both contained similar numbers of plastoglobules. In contrast to mesophyll chloroplasts, the bundle sheath chloroplasts possessed large starch granules that occupied the majority of chloroplast interior in nonsaline control plants, but the starch granules were thinner, occupied less of the chloroplast interior and were less numerous in the 200 mM NaCl treatment (Figure 5e,f).

3.4 | Distribution of suberin lamellae and plasmodesmata connections in bundle sheath cells

The cell walls of bundle sheath cells were thick and well developed with suberin lamellae visible as a dark band in the outer tangential and radial walls adjacent to mesophyll cells (Figure 6a,b). The suberin lamella was not observed at the interface of bundle sheath and xylem parenchyma cells (Figure 6c,d). Plasmodesmata were frequently observed between mesophyll and bundle sheath cells (Figure 6a,b), but were hardly observed between bundle sheath and xylem parenchyma cells (Figure 6c,d). There were no visible differences in suberization or frequency of plasmodesmata connections for bundle sheath cells in nonsaline and 200 mM treatments (saline treatment is shown in Figure 6 and nonsaline control in Figure S7).

The xylem parenchyma and phloem parenchyma cells each possessed a large central vacuole (Figure 7a,b) and the cytosol contained mitochondria and plastids located towards the cell periphery (Figure 7c,d). No differences were observed in the ultrastructure of xylem parenchyma and phloem parenchyma cells in the nonsaline

controls (Figure 7a,c) as compared with the 200 mM treatment (Figure 7b,d).

3.5 | Leaf-blade gas exchange, chlorophyll fluorescence and osmotic potential

Both salinity treatments did not affect the photosynthetic parameters relative to the nonsaline controls (Figure 8a–d). There were no differences in net photosynthetic rates (A), stomatal conductance (g_s), intercellular CO_2 concentrations (C_i) and chlorophyll fluorescence (F_v/F_m) between the control and the 100 and 200 mM NaCl treatments, with the average values of $29.4 \mu\text{mol CO}_2 \text{ m}^{-2} \text{ s}^{-1}$ for A , $0.18 \text{ mol H}_2\text{O m}^{-2} \text{ s}^{-1}$ for g_s , $120 \mu\text{mol CO}_2 \text{ mol}^{-1}$ for C_i and 0.78 for F_v/F_m . The water contents of the leaf-blades were on average 82% in nonsaline control and 100 mM NaCl treatments, but decreased to 79% in plants grown with 200 mM NaCl (Figure 8e). The leaf-blade sap osmotic potential was -0.92

MPa in nonsaline control and decreased to -1.2 MPa in 100 mM and -1.6 MPa in 200 mM NaCl treatments (Figure 8f).

4 | DISCUSSION

Our study demonstrates that leaf tissue tolerance to salinity in the monocotyledonous C_4 halophyte Rhodes grass is related to specific elemental distributions of Na and Cl, vacuolar compartmentation and

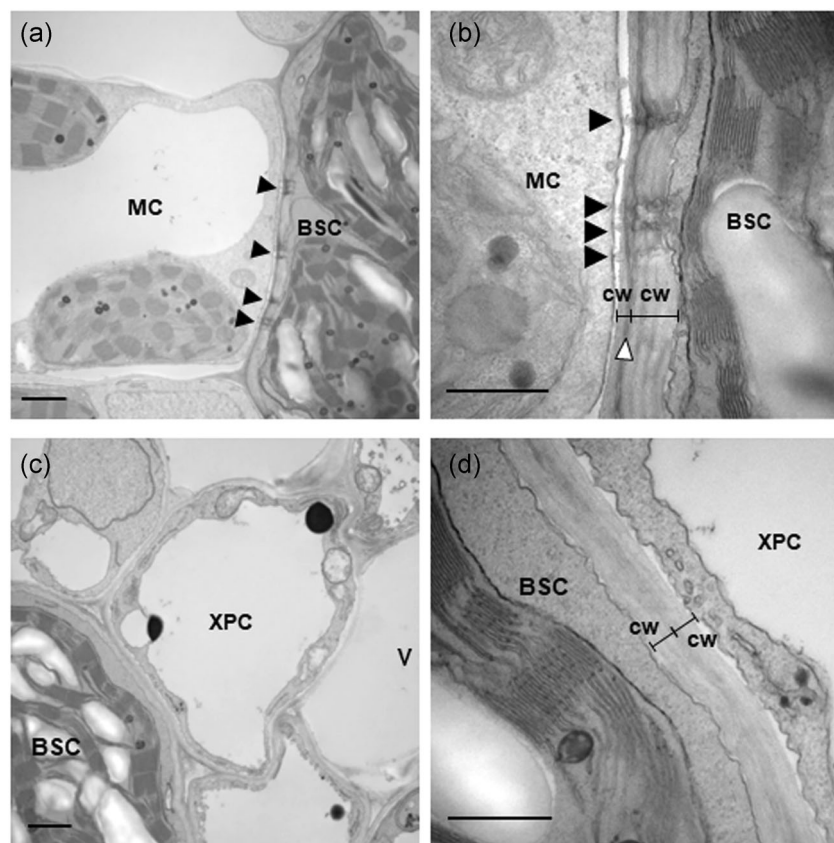
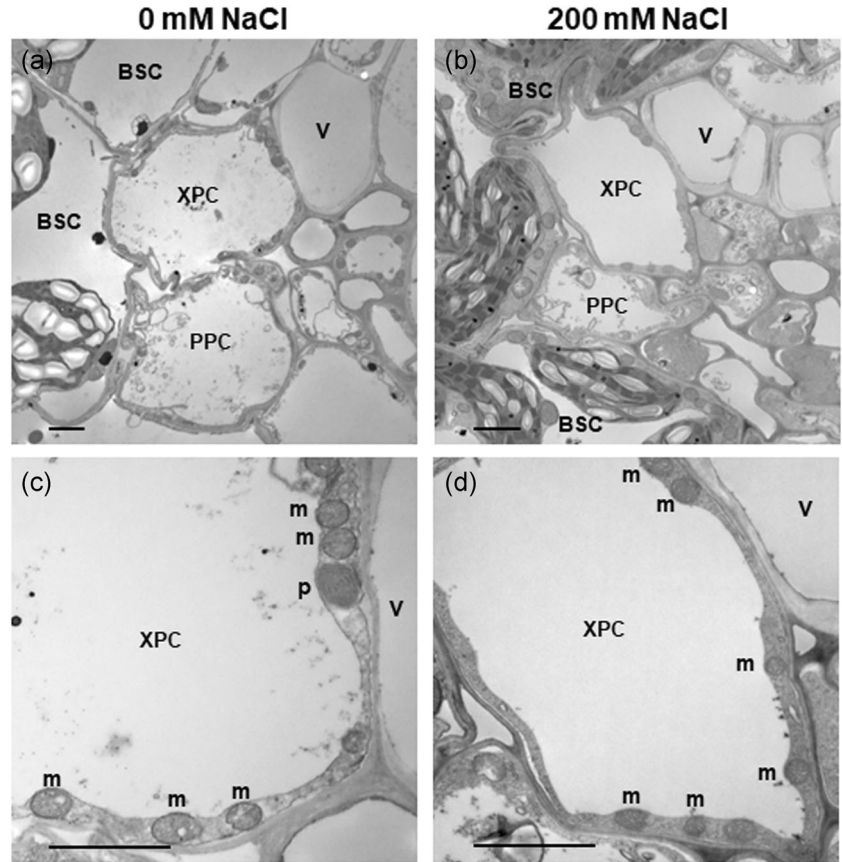


FIGURE 6 Transmission electron micrographs of cell walls at the interface between mesophyll and bundle sheath cells (a,b) and bundle sheath and xylem parenchyma (c,d) in the leaf-blade of the sixth leaves of Rhodes grass grown in aerated nutrient solution with 200 mM NaCl for 16 days. Treatments were imposed on 18-day-old plants. Images are typical of structure seen across three replicate leaves. There were no visible differences in suberization or frequency of plasmodesmata connections for bundle sheath cells in nonsaline (Figure S7) and 200 mM treatments. BSC, bundle sheath cell; cw, cell wall; MC, mesophyll cell; XPC, xylem parenchyma cell; V, vessel. Black arrowheads indicate plasmodesmata. White arrowhead indicates suberin lamellae in the cell wall of BSC. Scale bars = $1 \mu\text{m}$ (a,c) and $0.5 \mu\text{m}$ (b,d)

FIGURE 7 Transmission electron micrographs of vascular tissues in the leaf-blade of the sixth leaves of Rhodes grass grown in aerated nutrient solution with 0 (nonsaline control) (a, c) and 200 mM NaCl (b, d) for 16 days. Treatments were imposed on 18-day-old plants. Images are typical of structure seen across three replicate leaves. BSC, bundle sheath cell; m, mitochondrion; p, plastid; PPC, phloem parenchyma cell; XPC, xylem parenchyma cell; V, vessel. Scale bars = 2 μ m



the ability to maintain low levels of Na and Cl in chloroplasts of photosynthetically active bundle sheath cells. Below, we discuss the specific features of elemental distributions in the leaf tissues at the cellular level that include: (1) partitioning of Na and Cl into the xylem parenchyma; (2) restricted accumulation of Na and Cl in the photosynthetic sites, especially in bundle sheath chloroplasts; and (3) high accumulation of Ca in bundle sheath cells.

4.1 | Partitioning of Na and Cl into the xylem parenchyma

Xylem parenchyma cells accumulated the highest concentrations of Na (average of 529 mM) and Cl (average of 270 mM) among all leaf cell types when grown with 200 mM NaCl (Figures 2 and 3). In previous studies, the hypothesis of accumulation of Na in xylem parenchyma cells has relied mainly on measurements of tissue ion concentration or xylem sap extraction. In wheat, the withdrawal of Na from the xylem and accumulation of Na in the xylem parenchyma cells of leaf sheath have been suggested to reduce the delivery of Na to the leaf-blade (James et al., 2006a). In *Arabidopsis*, Sunarpi et al. (2005) showed that Na was loaded from the xylem into the xylem parenchyma cells of leaves by the AtHKT1 transporter that functions as a Na⁺ uniporter in the plasma membrane. This conclusion was based on the immunoelectron microscopy studies demonstrating the

presence of AtHKT1 in the plasma membrane of xylem parenchyma cells and an increase of Na concentration in the xylem sap of *athkt1* loss-of-function mutants. In the xylem parenchyma cells, Na could be sequestered into the vacuole by energy-dependent Na⁺/H⁺ antiporters in the tonoplast (Bassil et al., 2012). In the present study, we observed a large central vacuole and several mitochondria located in the cell periphery of xylem parenchyma (Figure 7c,d) that could provide energy to the 'proton pumps', which establish the H⁺ electrochemical gradient needed for secondary active ion transport processes (Munns et al., 2020). Although we could not resolve xylem ion concentrations due to difficulty in identifying xylem vessels in cryo-SEM-EDS maps, it has been previously reported that the Na concentration of xylem sap is about 10 mM in seven halophytes grown in nutrient solution with 200 mM NaCl (Rozema et al., 1981). Assuming that Na concentration in the xylem sap of Rhodes grass might be similar to this earlier report, this study shows the significant Na accumulation in the adjacent xylem parenchyma where it was ~500 mM in plants from the 200 mM treatment (Figure 3a). By contrast to Na, K concentrations in the xylem parenchyma cells during salinity treatment decreased to about 50% of those in non-saline control. This may indicate that xylem parenchyma extracts ions from xylem vessels and accumulate these in the vacuole selectively depending on the conditions. Taken together, xylem parenchyma of Rhodes grass could limit the transport of Na from the xylem to photosynthetic tissues (mesophyll and bundle sheath cells).

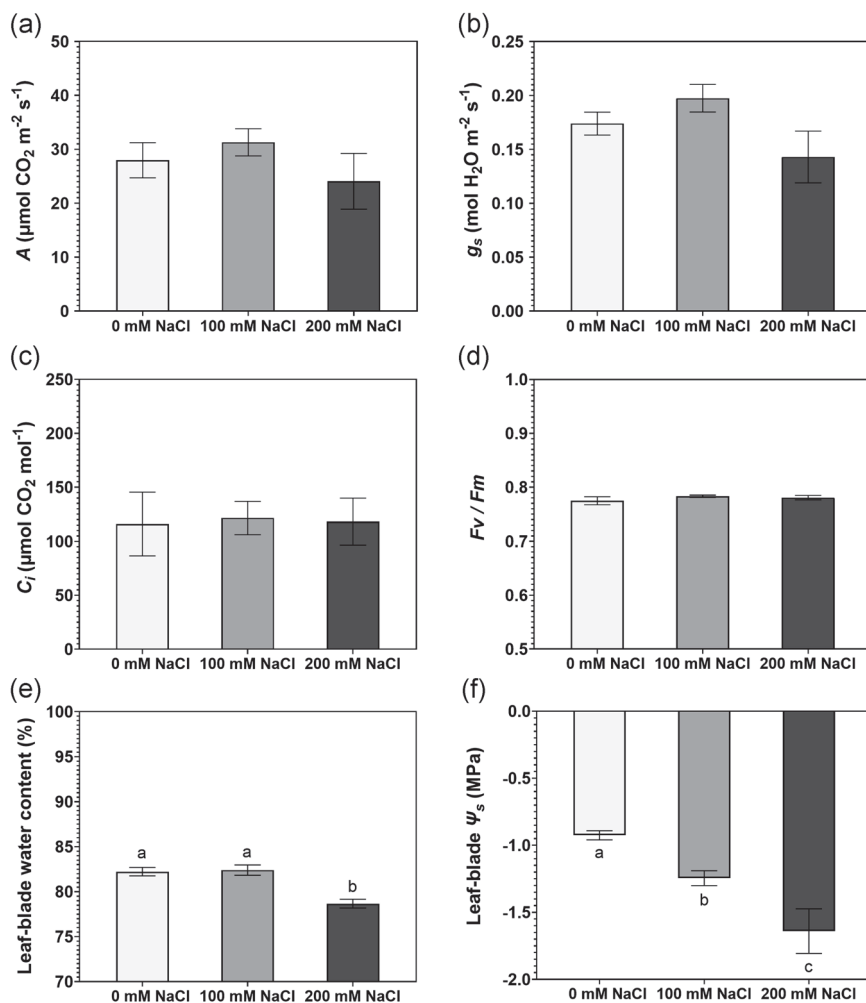


FIGURE 8 (a) Net photosynthetic rate (A), (b) stomatal conductance (g_s), (c) intercellular CO_2 concentration (C_i), (d) F_v/F_m , (e) leaf-blade water content and (f) leaf-blade osmotic potential (Ψ_s) of Rhodes grass grown in aerated nutrient solution with 0 mM (nonsaline control), 100 mM, or 200 mM NaCl for 16 days. Treatments were imposed on 18-day-old plants. Gas exchange parameters (a–c) were measured at a CO_2 concentration of $400 \mu\text{mol mol}^{-1}$. Data are means \pm SE of four replicates. Different letters indicate significant differences among treatments at $p < 0.05$ (Tukey's test)

4.2 | Partitioning of Na and Cl among epidermal, mesophyll and bundle sheath cells

Beyond the cells of the vascular tissues, the accumulation of Na and Cl was the highest in epidermal cells (382 and 138 mM, respectively), intermediate in mesophyll cells (307 and 76 mM, respectively) and the lowest in bundle sheath cells (195 and 34 mM, respectively) (Figure 3a,b). Previous studies reported on distributions of Na and/or Cl between the epidermal and mesophyll cells in leaves of salt-affected C_3 plants (in barley, Fricke et al., 1996, James et al., 2006b; in chickpea, Kotula et al., 2019).

The present study is the first data on cellular Na and Cl levels in a C_4 halophyte, Rhodes grass, which is characterized by specific Kranz anatomy; initial CO_2 fixation takes place in mesophyll cells and the Calvin cycle takes place in bundle sheath cells. Rhodes grass displays the preferential accumulation of Na in epidermal cells and maintains the lowest concentration of Na in bundle sheath cells, concurrent with decreased K concentration in epidermal and mesophyll cells and increased K levels in bundle sheath cells (Figure 3a,c). These cellular ion data indicate a redistribution of K from epidermis and mesophyll cells to bundle sheath cells. In addition to K redistribution, the ability to retain K in bundle sheath cells could have contributed to increased

K levels in these cells. The retention of K in photosynthetically active cells contributes to salinity tolerance in C_3 halophytes (Percey et al., 2016) and in barley (a relatively salt-tolerant C_3 nonhalophyte; Wu et al., 2015). As a result, the K:Na ratio of 32:1 in bundle sheath cells of Rhodes grass in the 200 mM NaCl treatment was similar to that in nonsaline controls (37:1) (Table 1). By contrast, the K:Na ratio decreased in leaf-blade epidermal cells of Rhodes grass from 166:1 in nonsaline control to 0.5:1 in the 200 mM NaCl treatment and in mesophyll cells from 173:1 to 0.6:1. Partitioning of elements by various cell types would depend on the rate of uptake and retention by cells, the capacity of vacuolar compartmentation or availability of ions to different cell types (Karley et al., 2000a).

We observed the highest concentrations of Na and Cl in xylem parenchyma cells of Rhodes grass, whereas Na and Cl were the lowest in the bundle sheath adjacent to xylem parenchyma and intermediate in mesophyll cells (Figures 2 and 3a,b). Several studies have suggested that the entry of solutes into bundle sheath cells is limited by the development of suberin lamellae in cell walls (Mertz & Bruntell, 2014). Suberin lamellae would isolate protoplasm from the apoplast and prevent taking up solutes from apoplastic space (Kotula et al., 2021). We observed suberin lamellae in the outer tangential walls of bundle sheath cells adjacent to mesophyll cells, partially in the radial walls between bundle

sheath cells, but not in the inner tangential walls at the interface between bundle sheath and xylem parenchyma cells (Figure 6a, b). Na (and other elements, e.g., Ca; see below) could enter the bundle sheath from xylem parenchyma through plasmodesmata (although the plasmodesmata connections were rare between these two cell types; Figure 6c) or via transporters in plasma membranes, but this could be limited by an intracellular Na-induced inhibition of instantaneous currents in the bundle sheath cells (Keunecke et al., 1997). The limitation of Na entry into the bundle sheath symplast would lead to the apoplastic movement of solutes with the transpiration stream through radial cell walls between suberin lamellae of adjacent bundle sheath cells (Mertz and Bruntell, 2014), leading to increased Na concentration in the apoplast of epidermis and mesophyll. The selective solute uptake from the apoplast by epidermis and mesophyll could then occur through regulation at the plasma membrane. Karley et al. (2000b) suggested that in barley preferential accumulation of Na from the apoplast into epidermal as compared to mesophyll cells could be due to differential regulation of instantaneously activating ion channels in the plasma membrane. In agreement with Karley et al. (2000b), we observed 1.2-fold higher concentrations of Na in epidermal as compared to mesophyll cells (Figure 3a). Once in the symplast, Na (and other elements) could enter the bundle sheath from mesophyll cells via multiple plasmodesmata connections (Figure 6a,b; Karley et al., 2000a), which are not blocked by suberin lamellae, and be sequestered in bundle sheath vacuoles.

4.3 | Na and Cl concentration in chloroplasts of mesophyll and bundle sheath cells

Concentrations of Na and Cl in chloroplasts of halophytes are regulated, with both ions being maintained at higher concentrations than in the leaves when grown in nonsaline conditions, but at much lower concentrations than in the leaves when grown in the presence of salt (Bose et al., 2017; Flowers et al., 2015; Robinson & Downton, 1985). Indeed, we observed about 2-fold higher concentrations of both Na and Cl in the chloroplasts than in the vacuoles of mesophyll cells in nonsaline control Rhodes grass, but not in bundle sheath cells (Figure 4a,b). The 200 mM NaCl treatment increased the concentrations of Na and Cl in both cell types, but the concentrations of Na in chloroplasts were 29% and 17% and the concentrations of Cl were 38% and 41% of those in vacuoles of mesophyll and bundle sheath cells, respectively (Figure 4a,b).

The chloroplasts in both mesophyll and bundle sheath cells did not show any structural damages (Figure 5). Indeed, net photosynthetic rates and the F_v/F_m were similar between the control and salinity treatments (Figure 8a,d). By contrast, swelling of thylakoids and disruption of envelopes were observed in salt-stressed C_3 nonhalophyte (e.g., chickpea, the ultrastructural changes in chloroplasts occurred at mesophyll cells Na concentration of ~220 mM; Kotula et al., 2019) or C_4 nonhalophytes (e.g., *Amaranthus tricolor*, *Panicum miliaceum*, *Sorghum bicolor*) or halophytes (e.g., *Chloris gayana*, *Cynodon dactylon*, *Eleusine coracana*) (Omoto et al., 2009, 2010). In studies by Omoto et al. (2009, 2010), ultrastructural changes in the

chloroplasts were observed in the mesophyll cells of plants treated with 3% NaCl (about 520 mM) per day for 5 days, but not in bundle sheath cells.

Maintenance of chloroplast ionic homeostasis is essential for ultrastructural integrity of chloroplasts and photosynthetic performance. In the present study, the chloroplastic concentration of Na and Cl in mesophyll cells increased from ~30 and ~15 mM, respectively, in plants from nonsaline solution to ~90 and ~30 mM, respectively, when plants were grown in 200 mM NaCl (Figure 4a,b). This charge imbalance ($Na^+ > Cl^-$) was overcome by the concurrent decrease in chloroplastic K concentration from ~200 mM in nonsaline solution to ~165 mM in 200 mM NaCl treatment (Figure 4c) and by the increase in P from ~50 mM in nonsaline solution to ~130 mM in the 200 mM NaCl treatment (Figure 4f), with P likely in the forms of $H_2PO_4^-$ (at pH ~6 such as in thylakoid lumen; Bose et al., 2017) or HPO_4^{2-} (at pH 8 such as in stroma; Bose et al., 2017). The chloroplastic concentrations of other elements (Ca, S; Figure 4d,e; Mg; Figure S6) remained similar in the nonsaline and 200 mM NaCl treatments.

The values of Na, Cl and K in chloroplasts of mesophyll cells obtained in the present study show similar changes in response to salinity as compared to those in chloroplasts of mesophyll cells of the C_3 succulent halophyte, *Suaeda maritima*, treated with 340 mM NaCl, that is, concentrations of Na and Cl increased and K decreased (Hajibagheri et al., 1984). Moreover, the chloroplastic Na concentrations in mesophyll cells of Rhodes grass (~90 mM for plants grown in 200 mM NaCl) are similar to Na concentrations in mesophyll chloroplasts of two C_3 halophytes, *Suaeda australis* and *S. maritima*, obtained using isolated chloroplasts or X-ray microanalysis, where Na concentration range was 84–115 mM in plants grown with 340–350 mM NaCl (Hajibagheri et al., 1984; Harvey et al., 1981; Robinson & Downton, 1985). Furthermore, in agreement with the results obtained for *Suaeda*, these chloroplastic concentrations of Na and Cl of salt-grown Rhodes grass are lower, and K is higher (Figure 4) than in the leaf tissue/sap (Figure S4a). Taken together, the results from the present and previous studies indicate that concentrations of Na, Cl and K in chloroplasts of halophytes are regulated for optimal functioning of chloroplasts.

4.4 | Cell-specific sequestration of Ca in leaf-blades

In contrast to Na and Cl, Ca was preferentially accumulated in the vacuole of bundle sheath cells of both nonsaline (708 mM) and saline (545 mM) plants, but in a lower concentration in epidermal cells, including bulliform cells, of nonsaline plants (160 mM) (Figures 2 and 3d). This distribution pattern of Ca is distinct from that of other monocots, where Ca accumulated almost exclusively in the epidermal cells and was low in mesophyll cells, or were present in bundle sheath cells (e.g., barley, Fricke et al., 1994, 1996; *Sorghum bicolor*, Boursier & Läuchli, 1989; reviewed in Conn & Gilliam, 2010). In eudicots, Ca predominantly accumulates in mesophyll and is low in epidermal and bundle sheath cells (e.g., *Citrus jambhiri*, Storey & Leigh, 2004; Conn & Gilliam, 2010), although this pattern is not consistent and may vary

extensively, even within a single family (e.g., Proteaceae; Guilherme-Pereira et al., 2018, Hayes et al., 2018). Karley et al. (2000a) suggested that cell-specific accumulation of Ca in barley is determined by the availability of Ca to different cell types as it moves in the apoplast with the transpiration stream (i.e., Ca transport from the xylem into epidermis via vein extension). Indeed, the proximity of bundle sheath cells to xylem vessels in Rhodes grass would expose these cells to high apoplastic Ca. More recently, however, several studies have indicated that selective accumulation of Ca arises from the ability of cells to take up Ca (i.e., expression of both Ca²⁺-permeable ion channels in the plasma membrane and Ca²⁺ transporters in the tonoplast; Hayes et al., 2018; Storey and Leigh, 2004), where it can accumulate to high concentrations (>700 mM in Rhodes grass). This selective accumulation of Ca could be linked: (i) to the allocation of Ca and P in different cell types, thus avoiding the precipitation of calcium phosphate that would reduce the availability of both nutrients and impact on the cellular process (P and Ca allocated to different cell types; Conn & Gilliam, 2010; Hayes et al., 2018, 2019, Ye et al., 2021) or (ii) to osmotic balance in specific cell types. The present study supports both assumptions: (i) P and Ca were localized in different cells (P-allocating epidermal and mesophyll cells did not accumulate Ca; see below) and (ii) high Ca concentration in bundle sheath cells may compensate for the low Na in the cells and thus contribute to charge and osmotic balance (Figures 2 and 3). Localized high concentrations of Ca (seen as white dots in the maps) are crystals, presumably Ca oxalates (Franceschi & Nakata, 2005), and were excluded from analyses.

4.5 | Accumulation of P (if present as a soluble anion) contributes to charge balance

The concentration of P was low in all cells analysed when plants were grown in nonsaline solution, but it increased to ~110 mM in epidermal cells and ~200 mM in bulliform and mesophyll cells in the ~240 mM NaCl treatment (Figure 3f). These results are in agreement with previous studies that showed increased P uptake and accumulation in leaves during salinity treatment (e.g., corn, Nieman & Clark, 1976; wheat, Munns & James, 2003). The increased accumulation of P, presumably in the form of H₂PO₄⁻ in vacuoles at pH 5.5 (Flowers et al., 2019), could assist to maintain charge balance for anions in addition to Cl⁻ (vacuolar concentration of Cl was only about 17% of the sum of Na and K concentrations in mesophyll cells and only about 8% in bundle sheath cells).

5 | CONCLUSIONS

We studied salt tolerance in Rhodes grass as a model for halophytic C₄ monocotyledonous species. We showed that tissue tolerance to salinity in Rhodes grass is related to cell-specific elemental distributions of Na and Cl, but also other elements (K, Ca, P, S) are partitioned among various cell types in leaf-blades in response to saline conditions. Our results support the hypothesis that preferential partitioning of Na, but also Cl in xylem parenchyma and epidermal cells, accounted for lower concentrations of Na and Cl in photosynthetically active mesophyll cells

and especially in bundle sheath cells. In addition to cellular partitioning of Na and Cl, Rhodes grass showed, as hypothesized, subcellular compartmentation with chloroplasts of mesophyll and bundle sheath cells maintaining Na and Cl at much lower concentrations than in the vacuoles of these cells for plants exposed to high salinity. No ultrastructural changes were observed in chloroplasts of either mesophyll or bundle sheath cells, and the photosynthetic activity was maintained. Specific accumulation of Ca in bundle sheath cells and P in epidermal, bulliform and mesophyll cells could have accounted for a charge or osmotic balance.

ACKNOWLEDGEMENTS

This study and Takao Oi was supported by the 2018 Australia Awards-Endeavour Fellowship of the Department of Education and Training, Australia, and was partially supported by the Japan Society for the Promotion of Science (JSPS) KAKENHI (JP19K15823 to Takao Oi). The authors acknowledge the use of the Microscopy Australia facilities at the Centre for Microscopy, Characterisation & Analysis, The University of Western Australia, a facility funded by the University, State and Commonwealth Governments. We also thank Carla Di Bella, Gustavo Striker and Yumika Watanabe for help with plant harvest, Wei Pei Ng for help with dry weight measurements, John Quealy for help with tissue ion analyses, Greg Cawthray for technical assistance in gas exchange and chlorophyll fluorescence measurements and Lyn Kirilak for cryo-SEM technical support. Open access publishing facilitated by The University of Western Australia, as part of the Wiley - The University of Western Australia agreement via the Council of Australian University Librarians.

CONFLICT OF INTERESTS

The authors declare that there are no conflict of interest.

DATA AVAILABILITY STATEMENT

The data that support the findings of this study are available from the corresponding author upon reasonable request.

ORCID

Takao Oi  <https://orcid.org/0000-0001-6664-849X>

Peta L Clode  <https://orcid.org/0000-0002-5188-4737>

Mitsutaka Taniguchi  <http://orcid.org/0000-0001-6485-2462>

Timothy D Colmer  <http://orcid.org/0000-0002-3383-9596>

Lukasz Kotula  <http://orcid.org/0000-0001-8760-7099>

REFERENCES

- Basu, P.S., Berger, J.D., Turner, N.C., Chaturvedi, S.K., Ali, M. & Siddique, K.H.M. (2007) Osmotic adjustment of chickpea (*Cicer arietinum*) is not associated with changes in carbohydrate composition of leaf gas exchange under drought. *Annals of Applied Biology*, 150, 217–225.
- Bassil, E., Coku, A. & Blumwald, E. (2012) Cellular ion homeostasis: emerging roles of intracellular NHX Na⁺/H⁺ antiporters in plant growth and development. *Journal of Experimental Botany*, 63, 5727–5740.
- Bose, J., Munns, R., Shabala, S., Gilliam, M., Pogson, B. & Tyerman, S.D. (2017) Chloroplast function and ion regulation in plants growing on saline soils: lessons from halophytes. *Journal of Experimental Botany*, 68, 3129–3143.

- Boursier, P. & Lauchli, A. (1989) Mechanisms of chloride partitioning in the leaves of salt-stressed *Sorghum bicolor* L. *Physiologia Plantarum*, **77**, 537–544.
- Cheeseman, J.M. (2013) The integration of activity in saline environments: problems and perspectives. *Functional Plant Biology*, **40**, 759–774.
- Conn, S. & Gilliam, M. (2010) Comparative physiology of elemental distributions in plants. *Annals of Botany*, **105**, 1081–1102.
- Flowers, T.J. & Colmer, T.D. (2008) Salinity tolerance in halophytes. *New Phytologist*, **179**, 945–963.
- Flowers, T.J., Glenn, E.P. & Volkov, V. (2019) Could vesicular transport of Na^+ and Cl^- be a feature of salt tolerance in halophytes? *Annals of Botany*, **123**, 1–18.
- Flowers, T.J., Munns, R. & Colmer, T.D. (2015) Sodium chloride toxicity and the cellular basis of salt tolerance in halophytes. *Annals of Botany*, **115**, 419–431.
- Franceschi, V.R. & Nakata, P.A. (2005) Calcium oxalate in plants: formation and function. *Annual Review of Plant Biology*, **56**, 41–71.
- Fricke, W., Leigh, R.A. & Tomos, A.D. (1994) Concentrations of inorganic and organic solutes in extracts from individual epidermal, mesophyll and bundle-sheath cells of barley leaves. *Planta*, **192**, 310–316.
- Fricke, W., Leigh, R.A. & Tomos, A.D. (1996) The intercellular distribution of vacuolar solutes in the epidermis and mesophyll of barley leaves changes in response to NaCl. *Journal of Experimental Botany*, **47**, 1413–1426.
- Guilherme Pereira, C., Clode, P.L., Oliveira, R.S. & Lambers, H. (2018) Eudicots from severely phosphorus-impooverished environments preferentially allocate phosphorus to their mesophyll. *New Phytologist*, **218**, 959–973.
- Hajibagheri, M.A., Harvey, D.M.R. & Flowers, T.J. (1984) Photosynthetic oxygen evolution in relation to ion contents in the chloroplasts of *Suaeda maritima*. *Plant Science Letters*, **34**, 353–362.
- Harvey, D.M.R., Hall, J.L., Flowers, T.J. & Kent, B. (1981) Quantitative ion localization within *Suaeda maritima* leaf mesophyll cells. *Planta*, **151**, 555–560.
- Hayes, P.E., Clode, P.L., Guilherme, Pereira, C. & Lambers, H. (2019) Calcium modulates leaf cell-specific phosphorus allocation in Proteaceae from south-western Australia. *Journal of Experimental Botany*, **70**, 3995–4009.
- Hayes, P.E., Clode, P.L., Oliveira, R.S. & Lambers, H. (2018) Proteaceae from phosphorus-impooverished habitats preferentially allocate phosphorus to photosynthetic cells: an adaptation improving phosphorus-use efficiency. *Plant, Cell & Environment*, **41**, 605–619.
- Hillel, D. (2000) Salinity management for sustainable irrigation: integrating science, environment, and economics. *Environmentally and socially sustainable development series*. Washington: The World Bank.
- James, R.A., Davenport, R.J. & Munns, R. (2006a) Physiological characterization of two genes for Na^+ exclusion in durum wheat, *Nax1* and *Nax2*. *Plant Physiology*, **142**, 1537–1547.
- James, R.A., Munns, R., von Caemmerer, S., Trejo, C., Miller, C. & Condon, A.G. (2006b) Photosynthetic capacity is related to the cellular and subcellular partitioning of Na^+ , K^+ and Cl^- in salt-affected barley and durum wheat. *Plant, Cell & Environment*, **29**, 2185–2197.
- Karley, A.J., Leigh, R.A. & Sanders, D. (2000a) Where do all the ions go? The cellular basis of differential ion accumulation in leaf cells. *Trends in Plant Science*, **5**, 465–470.
- Karley, A.J., Leigh, R.A. & Sanders, D. (2000b) Differential ion accumulation and ion fluxes in the mesophyll and epidermis of barley. *Plant Physiology*, **122**, 835–844.
- Keunecke, M., Sutter, J.U., Sattelmacher, B. & Hansen, U.P. (1997) Isolation and patch clamp measurements of xylem contact cells for the study of their role in the exchange between apoplast and symplast of leaf cells. *Plant and Soil*, **196**, 239–244.
- Kobayashi, H., Masaoka, Y., Takahashi, Y., Ide, Y. & Sato, S. (2007) Ability of salt glands in Rhodes grass (*Chloris gayana* Kunth) to secrete Na^+ and K^+ . *Soil Science and Plant Nutrition*, **53**, 764–771.
- Kotula, L., Clode, P.L., De La Cruz Jimenez, J. & Colmer, T.D. (2019) Salinity tolerance in chickpea is associated with the ability to 'exclude' Na from leaf mesophyll cells. *Journal of Experimental Botany*, **70**, 4991–5002.
- Kotula, L., Clode, P.L., Ranathunge, K. & Lambers, L. (2021) Role of roots in adaptation of soil-indifferent Proteaceae to calcareous soils in south-western Australia. *Journal of Experimental Botany*, **72**, 1490–1505.
- Kronzucker, H.J. & Britto, D.T. (2011) Sodium transport in plants: a critical review. *New Phytologist*, **189**, 54–81.
- Lipshitz, N., Shomer-Ilan, A., Eshel, A. & Waisel, Y. (1974) Salt glands on leaves of Rhodes grass (*Chloris gayana* Kth.). *Annals of Botany*, **38**, 459–462.
- Loch, D.S., Rethman, N.F.G. & vanNiekerk, W.A. (2004) Rhodegrass. In: Moser, L.E., Burson, B.L., Sollenberger, E.L., Al-Abmoodi, L.K., Barbarick, K.A., Roberts, C.A. & Dick W.A. (Eds.) *Warm season (C4) grasses*. Madison: American Society of Agronomy/Crop Science Society of America/Soil Science Society of America, pp. 833–872.
- Maathuis, F.J.M. & Amtmann, A. (1999) K^+ nutrition and Na^+ toxicity: the basis of cellular K^+/Na^+ ratios. *Annals of Botany*, **84**, 123–133.
- Marshall, A.T. (2017) Quantitative X-ray microanalysis of model biological samples in the SEM using remote standards and the XPP analytical model. *Journal of Microscopy*, **266**, 231–238.
- Mertz, R.A. & Brutnell, T.P. (2014) Bundle sheath suberization in grass leaves: multiple barriers to characterization. *Journal of Experimental Botany*, **65**, 3371–3380.
- Munns, R., Day, D.A., Fricke, W., Watt, M., Arsova, B., Barkla, B.J. et al. (2020) Energy costs of salt tolerance in crop plants. *New Phytologist*, **225**, 1072–1090.
- Munns, R. & James, R.A. (2003) Screening methods for salinity tolerance: a case study with tetraploid wheat. *Plant and Soil*, **253**, 201–218.
- Munns, R., James, R.A., Gilliam, M., Flowers, T.J. & Colmer, T.D. (2016) Tissue tolerance: an essential but elusive trait for salt-tolerant crops. *Functional Plant Biology*, **43**, 1103–1113.
- Munns, R. & Tester, M. (2008) Mechanisms of salinity tolerance. *Annual Review of Plant Biology*, **59**, 651–681.
- Munns, R., Wallace, P.A., Teakle, N.L. & Colmer, T.D. (2010) Measuring soluble ion concentrations (Na^+ , K^+ , Cl^-) in salt-treated plants. In: Sunkar, R. (Ed.) *Plant stress tolerance, methods and protocols*. New York: Humana Press, pp. 371–382.
- Negawo, A.T., Muktar, M.S., Assefa, Y., Hanson, J., Sartie, A.M., Habte, E. et al. (2021) Genetic diversity and population structure of a Rhodes grass (*Chloris gayana*) collection. *Genes*, **12**, 1233.
- Nieman, R.H. & Clark, R.A. (1976) Interactive effects of salinity and phosphorus nutrition on the concentrations of phosphate and phosphate esters in mature photosynthesizing corn leaves. *Plant Physiology*, **57**, 157–161.
- Oi, T., Hirunagi, K., Taniguchi, M. & Miyake, H. (2013) Salt excretion from the salt glands in Rhodes grass (*Chloris gayana* Kunth) as evidenced by low-vacuum scanning electron microscopy. *Flora*, **208**, 52–57.
- Oi, T., Taniguchi, M. & Miyake, H. (2012) Morphology and ultrastructure of the salt glands on the leaf surface of Rhodes grass (*Chloris gayana* Kunth). *International Journal of Plant Sciences*, **173**, 454–463.
- Omoto, E., Kawasaki, M., Taniguchi, M. & Miyake, H. (2009) Salinity induces granal development in bundle sheath chloroplasts of NADP-malic enzyme type C_4 plants. *Plant Production Science*, **12**, 199–207.
- Omoto, E., Taniguchi, M. & Miyake, H. (2010) Effects of salinity stress on the structure of bundle sheath and mesophyll chloroplasts in NAD-malic enzyme and PCK type C_4 plants. *Plant Production Science*, **13**, 169–176.
- Percey, W.J., Shabala, L., Wu, Q., Su, N., Breadmore, M.C., Rosanne Guijt, R.M. et al. (2016) Potassium retention in leaf mesophyll as an element of salinity tissue tolerance in halophytes. *Plant Physiology and Biochemistry*, **109**, 346–354.

- Robinson, S. & Downton, W. (1985) Potassium, sodium and chloride ion concentrations in leaves and isolated chloroplasts of the halophyte *Suaeda australis* R. Br. *Functional Plant Biology*, 12, 471–479.
- Rozema, J., Gude, H., Bijl, F. & Wesselman, H. (1981) Sodium concentration in xylem sap in relation to ion exclusion, accumulation and secretion in halophytes. *Acta Botanica Neerlandica*, 30, 309–311.
- Sage, R.F., Khoshravesh, R. & Sage, T.L. (2014) From proto-Kranz to C₄ Kranz: building the bridge to C₄ photosynthesis. *Journal of Experimental Botany*, 65, 3341–3356.
- Santos, J., Al-Azzawi, M., Aronson, J. & Flowers, T.J. (2015) eHALOPH a database of salt-tolerant plants: helping put halophytes to work. *Plant and Cell Physiology*, 57, e10.
- Shabala, S. (2013) Learning from halophytes: physiological basis and strategies to improve abiotic stress tolerance in crops. *Annals of Botany*, 112, 1209–1221.
- Shabala, S. & Pottosin, I. (2014) Regulation of potassium transport in plants under hostile conditions: implications for abiotic and biotic stress tolerance. *Physiologia Plantarum*, 151, 257–279.
- Storey, R. & Leigh, R.A. (2004) Processes modulating calcium distribution in citrus leaves. An investigation using X-ray microanalysis with strontium as a tracer. *Plant Physiology*, 136, 3838–3848.
- Sunarpi, Horie, T., Motoda, J., Kubo, M., Yang, H., Yoda, K. et al. (2005) Enhanced salt tolerance mediated by *AtHKT1* transporter induced Na⁺ unloading from xylem vessels to parenchyma cells. *The Plant Journal*, 44, 928–938.
- Suttie, J.M. (2000) *Hay and straw conservation: for small-scale farming and pastoral conditions*. No. 29; FAO Plant Production and Protection Series. Rome: Food and Agriculture Organization of the United Nations.
- Tester, M. & Davenport, R. (2003) Na⁺ tolerance and Na⁺ transport in higher plants. *Annals of Botany*, 91, 503–527.
- Wu, H., Zhu, M., Shabala, L., Zhou, M. & Shabala, S. (2015) K⁺ retention in leaf mesophyll, an overlooked component of salinity tolerance mechanism: a case study for barley. *Journal of Integrative Plant Biology*, 57, 171–185.
- Ye, D., Clode, P.L., Hammer, T.A., Pang, J., Lambers, H. & Ryan, M.H. (2021) Accumulation of phosphorus and calcium in different cells protect the phosphorus-hyperaccumulator *Ptilotus exaltatus* from phosphorus toxicity in high phosphorus soils. *Chemosphere*, 264, 128438.

SUPPORTING INFORMATION

Additional supporting information may be found in the online version of the article at the publisher's website.

How to cite this article: Oi, T., Clode, P.L., Taniguchi, M., Colmer, T.D. & Kotula, L. (2022) Salt tolerance in relation to elemental concentrations in leaf cell vacuoles and chloroplasts of a C₄ monocotyledonous halophyte. *Plant, Cell & Environment*, 45, 1490–1506. <https://doi.org/10.1111/pce.14279>